Compact fiber optic accelerometer

Feng Peng (彭 峰), Jun Yang (杨 军)*, Bing Wu (吴 冰), Yonggui Yuan (苑勇贵), Xingliang Li (李兴亮), Ai Zhou (周 爱), and Libo Yuan (苑立波)

Photonics Research Center, School of Science, Harbin Engineering University, Harbin 150001, China

**Corresponding author: yangjun141@263.net*

Received March 9, 2011; accepted June 3, 2011; posted online August 24, 2011

A compact fiber optic accelerometer based on a Michelson interferometer is proposed and demonstrated. In the proposed system, the sensing element consists of two single-mode fibers glued together by epoxy, which then act as a simple supported beam. By demodulating the optical phase shift, the acceleration is determined as proportional to the force applied on the central position of the two single-mode fibers. This simple model is able to calculate the sensitivity and the resonant frequency of the compact accelerometer. The experimental results show that the sensitivity and the resonant frequency of the accelerometer are 0.42 rad/g and 600 Hz, respectively.

OCIS codes: 120.3180, 060.2370, 130.3120, 120.7280.

doi: 10.3788/COL201210.011201.

In the past 20 years, significant progress has been achieved in the development of fiber optic accelerometers[1]. Recently, fiber optic accelerometers have been developed for a range of applications, including inertial navigation, earthquake monitoring, intruder detection, and machinery monitoring[2−6]. To make a small-sized fiber optic accelerometer, fiber Bragg grating (FBG)-based accelerometers have been proposed and developed[7−9]. Although FBG accelerometers have their own unique sensing capabilities, their sensitivity is less than that of interferometric fiber optic accelerometers. In addition, they are susceptible to variations in ambient temperature.

In this letter, a compact accelerometer based on Michelson interferometer is reported. This type of accelerometer integrates small size and lighter weight, and has all of the inherent advantages of fiber optic sensors.

The configuration of the acceleration sensing element is shown in Fig. 1. The compact acceleration-sensing element is composed of a solid frame and two parallel single-mode fibers that act as the sensing beam. Two single-mode fibers are glued together, and a mass is fixed onto the center of the sensing beam using epoxy. The sensing beam is inserted through two thin steel pipes, and the pipes are fixed at proper locations on the beam using epoxy. The steel pipes are then fixed on the solid frame using epoxy. When an external vibration is applied on the sensing beam, the optical path lengths of the two fibers change differently relative to the neutral surface (plane between the two fibers), resulting in an optical path difference between the two fibers. The accelerometer, which is activated by the external vibration, induces the optical phase shift of the two fibers. The variation of the optical phase shift is proportional to the accelerometer. The acceleration is thus obtained by demodulating the optical phase shift.

The configuration of the compact acceleration sensing system is presented in Fig. 2. The acceleration-sensing system consists of a single-mode all-fiber Michelson interferometer, a sensing element, and a phase-generated carrier (PGC) demodulation system. The interferometer is illuminated by a distributed feedback (DFB) tunable laser emitting at 1.55 μm with an output power of 1.6 mW. The optical beam is coupled onto the input end of a 3-dB single-mode fiber optic beam splitter, and is then divided and injected into two output fibers. The sensing element is coupled onto one of the two output fibers. The fiber distal end face of the sensing element, high-reflectance gold films are coated directly for use as reflecting mirrors. Consequently, the light is reflected back from the reflecting mirrors and recombined by the beam splitter. A PIN photodiode converts the interferometric intensity into an electric signal, which is subsequently processed by the PGC demodulation system[10].

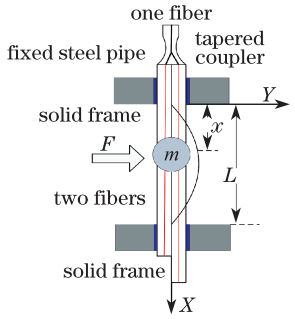

Fig. 1. Configuration of the sensing element.

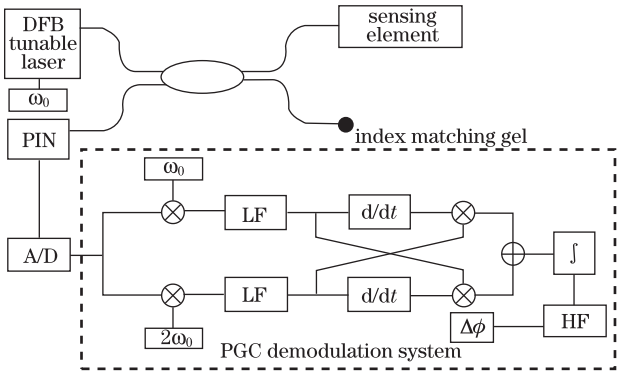

Fig. 2. Compact acceleration-sensing system based on a Michelson interferometer.

Fig. 3. Photo of the compact fiber optic accelerometer.

The package shell of the accelerometer in the proposed system is shown in Fig. 3. The shell is made of aluminum and is sufficiently stiff to maximize immunity to extraneous vibration. The diameter of the fiber optic accelerometer is 8 mm, and the length is 120 mm. The total weight does not exceed 20 g.

For the proposed interferometer optical setup, the optical phase shift in the sensing element induced by the vibration acceleration is analyzed. The optical phase shift in the fibers is determined by two factors: the fiber length change ΔL caused by the strain effect and the refractive index change Δn caused by the photoelastic effect, shown as[11]

$$\Delta\phi = 2\beta L\left[\frac{\Delta L}{L} + \frac{\Delta n}{n}\right], \tag{1}$$

where $\beta = 2\pi n/\lambda$ and $\lambda = 1\,550$ nm denotes the vacuum wavelength, $n = 1.458$ is the refractive index of the fiber core, L represents the effective length of the fiber, and Δn and ΔL represent the variation of the index and the core length between the two cores, respectively.

The factor of 2 in front of the right-hand side of the equation considers the fact that the light passes through the strained fiber section twice because of the reflective nature of the Michelson interferometer. From Eq. (1), the optical phase change can be deduced by[12]

$$\Delta\phi = 2\beta\Delta L\left\{1 - \frac{1}{2}n^2\left[(1-\mu)p_{12} - \mu p_{11}\right]\right\}, \tag{2}$$

where $p_{11} = 1.126$ and $p_{12} = 0.27$ are Pockels coefficients of the fiber, and $\mu = 0.17$ is the Poisson ratio of the fiber.

A simple analytical model is used to calculate the sensitivity and the resonant frequency of the fiber optic accelerometer.

Pick a microcell dl in any fiber core of the two sensing fibers. Then, $\Delta l/dl$ corresponding to the main strain component along X is given by[13]

$$\frac{\Delta l}{dl} = \frac{d}{R}, \tag{3}$$

where Δl is the length change of the micro cell, $d = 125$ μm is half the distance between the two cores, and R is the curvature radius of two bending fiber cores. From the mechanics of materials, R is given by

$$R = \frac{EI}{M_{\rm F}}, \tag{4}$$

where $E = 7.3 \times 10^{10}$ N/m^2 is the Young's modulus of the fiber; $I = 5\pi r_0^4/2$ and $M_{\rm F} = F \cdot x/2$ represent the inertia moment and the bending moment of the bending beam, respectively; $r_0 = 125$ μm is the radius of the fiber. By the Newton's second law, we have $F = Ma$, in which a is the vibration acceleration; $M = 17m'/35 + m$ is the total mass[14], including the mass of the two fibers $m' = \rho\pi r_0^2 2L$; $\rho = 2.28 \times 10^3$ kg/m^3 is the density of the fiber, and m is the loading mass.

Substituting Eq. (3) into Eq. (4), the variation of the core length between the two cores ΔL is given by

$$\Delta L = 4\int_0^{L/2} \frac{xd}{2EI} F\mathrm{d}x = \frac{dL^2}{4EI}F. \tag{5}$$

Inserting Eq. (5) into Eq. (2), the accelerometer sensitivity $\Delta\phi/a$ can be expressed as

$$\frac{\Delta\phi}{a} = \frac{\pi n d L^2}{\lambda EI}\left\{1 - \frac{1}{2}n^2\left[(1-\mu)p_{12} - \mu p_{11}\right]\right\}M. \tag{6}$$

The resonance frequency of the accelerometer $f_{\rm n}$ is given by

$$f_{\rm n} = \frac{1}{2\pi}\left(\frac{K}{M}\right)^{1/2} = \frac{1}{2\pi}\left[\frac{96EI}{(\frac{17}{35}m' + m)L^3}\right]^{1/2}, \tag{7}$$

where K is the stiffness coefficient of the two sensing fibers.

To investigate the performance of the compact fiber optic accelerometer, a testing system is established for measuring the vibration acceleration, as shown in Fig. 4. The solid frame, including the compact fiber optic accelerometer, is vertically mounted onto a vibration stage, and a piezoelectric accelerometer is vertically mounted on the frame near the fiber accelerometer for calibrating.

The amplitude of the output signal of the accelerometer is monitored during the process of carefully rotating the fiber accelerometer. When the amplitude of the signal reaches maximum, the applied force can be considered parallel to the plane of the two cores and perpendicular to the fiber axis; the fiber accelerometer measures the same component of acceleration as the piezoelectric accelerometer. In addition, all of the other experimental setups are fixed on a vibration insulation table to prevent impacts from external vibration.

In the compact fiber optic accelerometer, the effective length L of the two fibers is 5 cm, and there is no loading

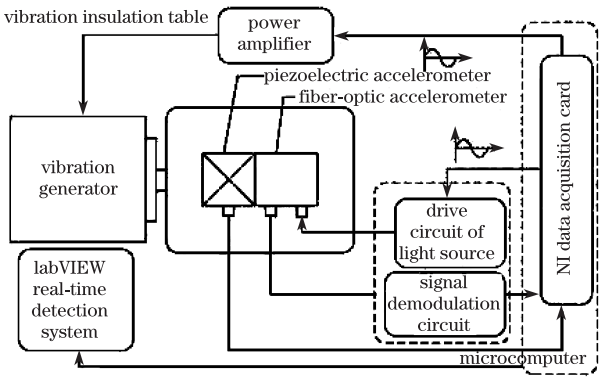

Fig. 4. Testing system of the compact fiber optic accelerometer.

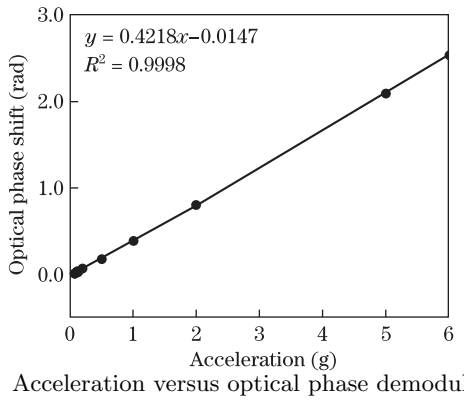

Fig. 5. Acceleration versus optical phase demodulation.

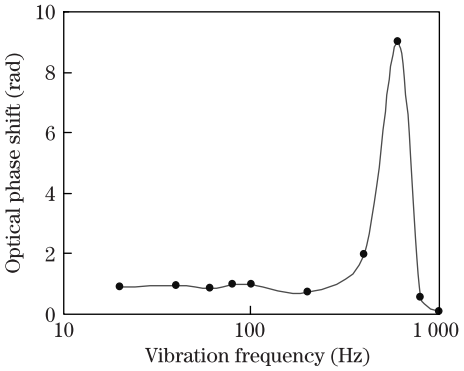

Fig. 6. Amplitude-frequency characteristic.

($m = 0$) on the fiber. Figure 5 shows the detected optical phase shift versus acceleration of the accelerometer when the vibration frequency is 50 Hz. The experimental result gives a good linearity response between the optical phase shift and the acceleration. From the slope of the trend line, the sensitivity of the accelerometer is 0.42 rad/g. The amplitude-frequency characteristic is presented in Fig. 6, which shows that the resonant frequency of the fiber optic accelerometer is 600 Hz, and the available frequency range is 0–320 Hz, where the frequency fluctuation range is less than 3 dB.

The theoretical acceleration sensitivity and resonance frequency are 0.28 rad/g from Eq. (6) and 708 Hz from Eq. (7), respectively. According to Figs. 5 and 6, respectively, the measured sensitivity is 0.42 rad/g and the resonant frequency is 600 Hz. This is because all the values taken in the theoretical calculation are ideal numbers. The condition that the two single-mode fibers are glued together with epoxy, which introduces an additional mass to the fiber probe, is not considered in the theoretical calculation. According to Eqs. (6) and (7), respectively, the sensitivity is directly proportional to the total mass and the resonant frequency is inversely proportional to the square root of the total mass. Therefore, an increase in the mass leads to an increase in sensitivity and a decrease in the resonant frequency.

Based on this proportional relation, when the sensitivity is 0.42 rad/g, the corresponding resonant frequency is 578 Hz. Compared with the measured frequency, the experimental error is within 5% of the anticipated value obtained from numerical analysis. Consequently, the measured results are qualitatively consistent with the theoretical prediction.

In conclusion, a compact accelerometer based on Michelson interferometer is demonstrated. The performance of the fiber optic accelerator shows that such an accelerometer has a sensitivity of 0.42 rad/g and a resonant frequency of 600 Hz. The accelerometer is more compact and lighter. In addition, the accelerometer is temperature-insensitive due to the two sensing fibers being glued together. When the temperature changes, each fiber changes. Thus, the optical phase change caused by the ambient temperature fluctuation is automatically compensated.

This work was partially supported by the National Nature Science Foundation of China (Nos. 60877046, 60707013, 60807032, and 60927008), the Key Project of the Nature Science Foundation of Heilongjiang Province (No. ZD200810), and the Fundamental Research Funds for the Central Universities (No. HEUCFZ1020).

References

1. M. D. Todd, G. A. Johnson, B. A. Althouse, and S. T. Vohra, IEEE. Photon. Technol. Lett. **10,** 1605 (1998).
2. B. Wu, C. Chen, G. Ding, D. Zhang, and Y. Cui, Opt. Eng. **43,** 313 (2004).
3. R. I. Crickmore, P. J. Nash, and J. P. F. Wooler, Proc. SPIE **5611,** 79 (2004).
4. D. A. Jackson, Meas. Sci. Technol. **20,** 34010 (2009).
5. Q. Wang and Q. Yu, Chin. Opt. Lett. **8,** 266 (2010).
6. F. Qin, H. Li, W. Fan, and Q. Sheng, Chin. Opt. Lett. **7,** 556 (2009).
7. J. Wang, T. Liu, C. Wang, X. Liu, D. Huo, and J. Chang, Meas. Sci. Technol. **21,** 094012 (2010).
8. A. Laudati, F. Mennella, M. Giordano, G. D. Altrui, C. C. Tassini, and A. Cusano, IEEE. Photon. Technol. Lett. **19,** 1991 (2007).
9. G. Gagliardi, M. Salza, P. Ferraro, P. De Natale, A. Di Maio, S. Carlino, G. De Natale, and E. Boschi, Meas. Sci. Technol. **19,** 085306 (2008).
10. A. Dandridge, A. B. Tveten, and T. G. Giallorenzi, IEEE. J. Quantum Electron. **18,** 1647 (1982).
11. L. Yuan, J. Yang, Z. Liu, and J. Sun, Opt. Lett. **31,** 2692 (2006).
12. A. S. Gerges, T. P. Newson, J. D. C. Jones, and D. A. Jackson, Opt. Lett. **14,** 251 (1989).
13. L. Yuan, J. Yang, and Z. Liu, IEEE. Sens. J. **8,** 1114 (2008).
14. B. Wen, *Theory of Mechanical Vibration and Its Application* (in Chinese) (High Education Press, Beijing, 2009).
15. C. M. Harris and A. G. Piersol, *Harris' Shock and Vibration Handbook* (in Chinese) S. Liu, J. Wang, F. Li, J. Long, and W. Shi (trans). (China Petrochemical Press, Beijing, 2008).